arXiv:1405.5105v4 [cond-mat.mes-hall] 30 Jun 2015

Size Effects in Thermal Conduction by Phonons

Philip B. Allen[1,*]

[1] *Physics and Astronomy Department, Stony Brook University, Stony Brook, NY 11794-3800, USA*

(Dated: July 1, 2015)

Heat transport in nanoscale systems is both hard to measure microscopically, and hard to interpret. Ballistic and diffusive heat flow coexist, adding confusion. This paper looks at a very simple case: a nanoscale crystal repeated periodically. This is a popular model for simulation of bulk heat transport using classical molecular dynamics (MD), and is related to transient thermal grating experiments. Nanoscale effects are seen in perhaps their simplest form. The model is solved by an extension of standard quasiparticle gas theory of bulk solids. Both structure and heat flow are constrained by periodic boundary conditions. Diffusive transport is fully included, while ballistic transport by phonons of long mean free path is diminished in a specific way. Heat current $J(x)$ and temperature gradient $\nabla T(x')$ have a non-local relationship, *via* $\kappa(x-x')$, over a distance $|x-x'|$ determined by phonon mean free paths. In MD modeling of bulk conductivity, finite computer resources limit system size. Long mean free paths, comparable to the scale of heating and cooling, cause undesired finite-size effects that have to be removed by extrapolation. The present model allows this extrapolation to be quantified. Calculations based on the Peierls-Boltzmann equation, using a generalized Debye model, show that extrapolation involves fractional powers of $1/L$. It is also argued that heating and cooling should be distributed sinusoidally ($\dot{e} \propto \cos(2\pi x/L)$) to improve convergence of numerics.

PACS numbers: 66.70.-f, 63.22.-m, 65.80.-g

I. INTRODUCTION

The linear relation between heat current $\vec{J}$ and temperature gradient $\vec{\nabla} T$ is

$$J_\alpha(\vec{r}) = -\int d\vec{r}' \kappa_{\alpha,\beta}(\vec{r},\vec{r}')\nabla_\beta T(\vec{r}'). \quad (1)$$

This non-local expression[1] defines the general linear response for a time-independent (steady state) heat flow. This paper concerns cases where heat flows in a single (x) direction in response to a temperature gradient in the same direction. Then the spatial variation of $\vec{J}$, $\vec{\nabla} T$, and κ can be simplified by averaging over y and z directions. The conductivity $\kappa_{\alpha,\beta}(\vec{r},\vec{r}')$ becomes the scalar $\kappa(x,x')$,

$$J_x(x) = -\int dx' \kappa(x,x')\nabla_x T(x'). \quad (2)$$

When the distance scale of variation of the temperature gradient is longer than the carrier mean-free path Λ, a local approximation (the usual Fourier law $J_x = -\kappa_0 \nabla_x T$) works. This is the usual situation in a macroscopic measurement on a spatially homogeneous sample; the temperature gradient typically has negligible spatial variation on the scale of Λ. In this limit, $\kappa(x,x') = \kappa(x-x')$, and $\kappa_0 = \int dx \kappa(x)$. In the homogeneous case, assuming a long sample, Fourier variables are appropriate. The linear relation is then $J_x(k) = -\kappa(k)\nabla_x T(k)$. I will use the same symbol ($\nabla_x T$ for example) to indicate both coordinate space and reciprocal space representations of functions, the coordinate x or k being explicitly shown. For a homogeneous sample and constant temperature gradient, the experiment is described by the $k = 0$ Fourier component, and $\kappa_0 = \lim_{k\to 0} \kappa(k)$.

Nanoscale systems have boundaries that add complexity[2–5]. There is an argument[6] that says the generalized Fourier law Eq.(1) does not apply in all cases. This paper avoids such issues, and addresses a case where the complexity is minimized, namely, a homogeneous nanoscale system with periodic boundary conditions. This geometry is experimentally realized in transient thermal grating experiments[7–9]. It is also a preferred geometry for simulation of heat transport by classical molecular dynamics (MD) using the "direct method"[10–14]. Heat is introduced locally, extracted locally some distance away, and temperature is monitored in between. The aim of the modeling is usually to extract the conductivity of a macroscopic sample. Nanoscales automatically enter, because the computer cannot process atomic information on a macroscopic scale.

A very nice example was given by Zhou *et al.*[13], who carefully analyze computational accuracy, using the semiconductor GaN as an example. The large thermal conductivity (several hundred W/mK at room temperature) indicates that the dominant acoustic phonons have mean free paths Λ_Q of order hundreds of interatomic spacings a. Since acoustic-phonon mean-free paths increase rapidly as wave-vector $\vec{Q} \to 0$, significant heat is carried by phonons with much longer mean free paths, thousands in units of a. The simulations were done for periodic cells up to length $L \approx 1000a$. Probably another factor of 10 in length would be required to fully converge the answers. At a series of lengths $L < 1000a$, conductivity $\kappa_{\rm eff}(L)$ was extracted as the ratio $-J_x/\nabla_x T$, where the temperature gradient was determined at $x = \pm L/4$, half way between the heat source and sink. Extrapolation of

$\kappa_{\rm eff}(L)$ to $L \to \infty$ (assuming $\kappa_{\rm eff}(L) - \kappa_{\rm bulk} \propto 1/L$) indicated that the value of $\kappa_{\rm bulk}$ was typically twice bigger than the maximum achieved value $\kappa_{\rm eff}(L \approx 1000a)$. Zhou *et al.*[13] discover evidence of a breakdown in this method of extrapolation. The breakdown was analyzed by Sellan *et al.*[15]; the alternate analysis given here uses similar Debye-model simplifications, but different boundary assumptions. Both offer ways of improving extrapolation needed in MD computation of κ.

The simplicity of the periodic boundary means that phonon gas theory can be easily adapted to this nanoscale situation. Here I offer such an analysis. The result supports the idea of Sellan *et al.*[15] that $\kappa_{\rm eff}(L) - \kappa_{\rm bulk} \propto 1/\sqrt{L}$ should give a better extrapolation. The analysis also points to a better algorithm for adding and removing heat.

II. SEGMENTED PERIODIC SLAB MODEL

Fig. 1 is a cartoon system ("simulation cell") of N "slabs," each of width d, corresponding to a total length $L = Nd$. The system is repeated periodically, as sometimes used in classical MD simulations. The primary variables are the imposed rate of heating per unit volume, $\dot{e}(\ell)$, of the ℓ'th slab, and the "measured" slab temperature $T(\ell)$ (mean kinetic energy of the atoms in the slab, divided by $3k_B/2$). These primary variables coincide with the quantities measured in heat conduction experiments. The secondary variables are the heat flux $J_x(\ell+\frac{1}{2})$ and the temperature gradient $\nabla_x T(\ell+\frac{1}{2})$; both are defined at the junction of slabs ℓ and $\ell+1$. The secondary variables are related to the primary variables by the two fundamental slab-ring equations,

$$\nabla_x T(\ell+\frac{1}{2}) = [T(\ell+1) - T(\ell)]/d \tag{3}$$

$$\dot{e}(\ell) = [J_x(\ell+\frac{1}{2}) - J_x(\ell-\frac{1}{2})]/d \tag{4}$$

Equation 4 is energy conservation. To allow a steady state, it is required that $\sum_\ell \dot{e}(\ell) = 0$, meaning that no net heating occurs.

The relation between heat flux and temperature gradient, in linear approximation, is

$$J_x(\ell+\frac{1}{2}) = -\sum_{m=0}^{N-1} \kappa(\ell-m)\nabla_x T(m+\frac{1}{2}) \tag{5}$$

This is the analog of Eq.(2). The position variable x has been discretized into the slab index ℓ. The thermal conductivity is similarly discretized. In terms of these discrete and periodic variables, the form of Eq.(5) is required by the linear approximation. The matrix $\kappa(\ell, m)$ is rigorously defined. It is independent of the heating $\dot{e}(\ell)$. If the slabs are identical, then $\kappa(\ell, m)$ retains the

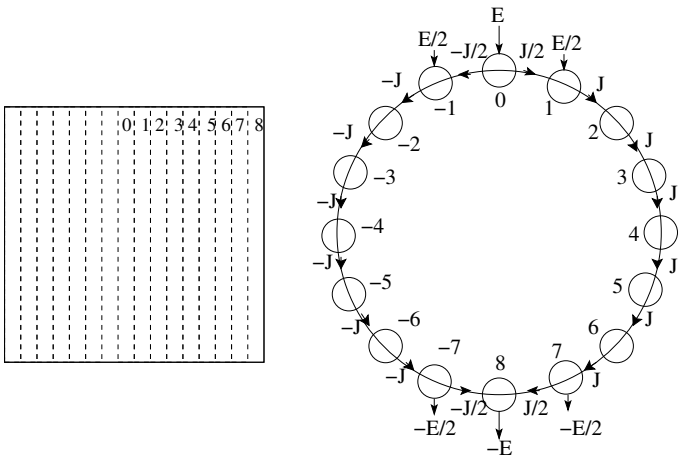

FIG. 1. Two schematics of a periodic supercell used for MD modeling of thermal conductivity. The cell is divided into N slabs (here $N = 16$) in the direction x of heat flow. It is periodically repeated in all three directions. Heat is randomly inserted as impulses on randomly chosen atoms in slab 0. Equal random extraction of heat occurs in slab $N/2$. Thus the heat current density J is controlled. Temperature is measured in slabs $1, 2, \ldots, N/2-1$, and also in the similar slabs $-1, -2, \ldots$. The temperature gradient dT/dx is minimum in slab $N/4$ and $3N/4$. From these gradients, the value of $\kappa_{\rm eff}(N) = J/|dT/dx|_{\rm min}$ is evaluated.

N-fold translational symmetry of the ring. Therefore $\kappa(\ell+n, m+n) = \kappa(\ell, m) = \kappa(\ell-m, 0) \equiv \kappa(\ell-m)$. All variables are N-fold periodic in ℓ, including the nonlocal conductivity $\kappa(\ell) = \kappa(\ell+N)$.

Conjugate to the N positions on the ring are N Fourier vectors $q = (2\pi/L)n_q$, with $L = Nd$ and n_q defined *modulo* N. I will always use k for the Fourier transform of the continuous variable x, and q for the discrete case. This notation then clarifies that $\kappa(k)$ refers to thermal conductivity of a large homogeneous system, and $\kappa(q)$ to the small but periodically repeated supercell.

Just as the integers ℓ are defined *modulo* N, similarly the integers n_q have the same periodicity, $n_q + N = n_q$. The Fourier representation of the discretized variables is particularly simple and convenient:

$$\begin{aligned}
\dot{e}(\ell) &= \sum_q e^{iqd\ell}\dot{e}(q) \\
T(\ell) &= \sum_q e^{iqd\ell}T(q) \\
J_x(\ell+\frac{1}{2}) &= \sum_q e^{iqd(\ell+\frac{1}{2})}J_x(q) \\
\nabla_x T(\ell+\frac{1}{2}) &= \sum_q e^{iqd(\ell+\frac{1}{2})}\nabla_x T(q) \\
\kappa(\ell) &= \sum_q e^{iqd\ell}\kappa(q),
\end{aligned} \tag{6}$$

where sums go over the N distinct values of q. The re-

verse transforms are

$$\dot{e}(q) = \frac{1}{N}\sum_{\ell} e^{-iqd\ell}\dot{e}(\ell)$$
$$J_x(q) = \frac{1}{N}\sum_{\ell} e^{-iqd(\ell+\frac{1}{2})}J_x(\ell+\frac{1}{2}), \qquad (7)$$

and similar for T, $\nabla_x T$, and κ. Sums go over the N distinct values of ℓ. The reciprocal space version of Eq.(5) is

$$J_x(q) = -\kappa(q)\nabla_x T(q) \qquad (8)$$

III. PHONON GAS THEORY

This section assumes a macroscopic homogeneous ("continuum") solid. The next section translates this to a segmented supercell of periodic ("discrete") slabs. The short-hand Q, in both continuum and discrete models, denotes $(\vec{Q}, s)$, the (three-dimensional) wavevector $\vec{Q}$ and the branch index s of the phonons. Spatial variation is driven by external heating and is assumed to occur only in the x direction. Thermal properties are described by $N_Q(x)$, the mean occupation of mode Q at (one-dimensional) position x. The heat current is

$$J_x(x) = \frac{1}{\Omega}\sum_{Q} \hbar\omega_Q v_{Qx} N_Q(x), \qquad (9)$$

The Peierls-Boltzmann equation (PBE)[16,17] describes the dynamics of $N_Q(x)$. Anharmonic phonon events drive N_Q to the local thermal equilibrium Bose-Einstein distribution $n_Q = 1/(\exp(\hbar\omega_Q/k_B T(x)) - 1)$. Spatial variations in $N_Q(x,t)$ change by phonon drift with velocity $\vec{v}_Q = \partial\omega_Q/\partial\vec{Q}$. In steady state, N_Q is stationary,

$$\frac{\partial N_Q}{\partial t} = 0 = \left(\frac{\partial N_Q}{\partial t}\right)_{\text{drift}} + \left(\frac{\partial N_Q}{\partial t}\right)_{\text{collisions}}. \qquad (10)$$

Writing N_Q as the sum of a local equilibrium $n_Q(T(x))$ (unaffected by collisions) and a deviation $\Phi_Q(x)$, the drift term of the PBE has two contributions, $-(\partial n_Q/\partial T)v_{Qx}\nabla_x T$ and $-v_{Qx}\nabla_x\Phi_Q$. The second of these vanishes when the temperature gradient is constant, but becomes important when there is spatial inhomogeneity. The collision term, after linearization, has the form $-\sum_{Q'} C_{QQ'}\Phi_{Q'}$, where $C_{QQ'}$ is a complicated collision operator. To first approximation (the "relaxation time approximation," RTA) this can be written as $-\Phi_Q/\tau_Q$, where $1/\tau_Q$ is the "single mode relaxation rate," meaning the thermalization rate (or life-time broadening) of mode Q that appears if only that one mode is out of equilibrium. The PBE then takes the form

$$[v_{Qx}\nabla_x + 1/\tau_Q]\Phi_Q(x) = -v_{Qx}\frac{\partial n_Q}{\partial T}\nabla_x T \qquad (11)$$

In the continuum picture, the direct and reciprocal-space representations are related by $\Phi_Q(x) = (1/2\pi)\int dk \exp(ikx)\Phi_Q(k)$ and $\Phi_Q(k) = \int dx \exp(-ikx)\Phi_Q(x)$. The PBE becomes

$$(ikv_{Qx} + 1/\tau_Q)\Phi_Q(k) = -v_{Qx}\frac{\partial n_Q}{\partial T}\nabla_x T(k). \qquad (12)$$

The thermal conductivity $\kappa(k)$ in continuous k space obeys the reciprocal-space version of Eq.(2), $J_x(k) = -\kappa(k)\nabla_x T(k)$, and has the form

$$\kappa(k) = \frac{1}{\Omega}\sum_{Q} \frac{\hbar\omega_Q v_{Qx}^2(\partial n_Q/\partial T)}{1/\tau_Q + ikv_{Qx}} \qquad (13)$$

This can be Fourier-transformed back to x-space:

$$\kappa(x-x') = \frac{1}{\Omega}\sum_{Q}^{v_{Qx}>0} \hbar\omega_Q v_{Qx}\frac{\partial n_Q}{\partial T}\exp\left[-\frac{|x-x'|}{\Lambda_{Qx}}\right], \qquad (14)$$

where the mean free path is $\Lambda_{Qx} = v_{Qx}\tau_Q$. This uses the property that v_{Qx} and Λ_{Qx} change sign when $\vec{Q}$ changes sign.

The result Eq.(14) shows explicitly that heat transport is influenced non-locally by temperature variations. The velocity $|v_{Qx}|$ is bounded, but the mean free path $\Lambda_{Qx} = v_{Qx}\tau_Q$ is not. Relaxation times of long wavelength acoustic phonons diverge as $|\vec{Q}| \to 0$. In the oversimplified ("gray") model where every phonon Q has the same relaxation rate $1/\tau_Q = 1/\tau_0$, the Q-integrated $\kappa(x)$ decays rapidly. But because the spatial decay rate in Eq.(14) involves $1/\Lambda_0|\cos\theta_Q|$, no simple exponential formula works. The decay is more rapid than the simple exponential $\exp(-|x|/\Lambda_0)$. However, in more realistic models, the divergence of τ_Q and Λ_{Qx} at small Q causes, after Q-integration, a slower than exponential decay. Still, in Eq.(14), even long-wavelength phonons are diffusive because the sample is "macroscopic."

IV. GAS THEORY ON THE SEGMENTED PERIODIC SLAB

Gas theory translates to the segmented supercell in a slightly awkward way. Temperature $T(\ell)$ is a slab property, but current $J_x(\ell+\frac{1}{2})$ is a junction property. Gas theory has temperature as a primary variable, so $T(\ell)$ should correspond to $T(x)$ averaged over the ℓ'th slab. Evidently $N_Q(\ell)$ is a slab property, not a junction property. But since the current in gas theory is $\sum_Q \hbar\omega_Q v_{Qx} N_Q/\Omega$, we are forced to compromise and define

$$J_x(\ell+\frac{1}{2}) = \frac{1}{\Omega}\sum_{Q} \hbar\omega_Q v_{Qx}\frac{N_Q(\ell) + N_Q(\ell+1)}{2}. \qquad (15)$$

Transforming to the discrete slab Fourier representation, this becomes

$$J_x(q) = \frac{1}{\Omega}\sum_Q \hbar\omega_Q v_{Qx}\cos(qd/2)\Phi_Q(q). \quad (16)$$

Similarly, the temperature gradient, Eq.(3), in Fourier variables, is

$$\nabla_x T(q) = 2i\sin(qd/2)T(q)/d, \quad (17)$$

and the fundamental connection Eq.(4) between heat input and current is

$$\dot{e}(q) = 2i\sin(qd/2)J_x(q)/d. \quad (18)$$

The remaining task is to translate Eq.(13) to slab language. The ingredient needing translation is ∇_x which appears twice in Eq.(11). The translation of this equation is

$$\begin{aligned}\Phi_Q(\ell) &= \theta(v_{Qx})v_{Qx}\tau_Q/d \\ &\times\left[\frac{\partial n_Q}{\partial T}(T(\ell-1)-T(\ell)) + (\Phi_Q(\ell-1)-\Phi_Q(\ell))\right] \\ &+ \theta(-v_{Qx})v_{Qx}\tau_Q/d \\ &\times\left[\frac{\partial n_Q}{\partial T}(T(\ell)-T(\ell+1)) + (\Phi_Q(\ell)-\Phi_Q(\ell+1))\right],\end{aligned} \quad (19)$$

where $\theta(x)$ is the unit step function. The meaning is that drift entering slab ℓ from the left uses positive velocity phonons which carry information from the slab on the left, while drift entering slab ℓ from the right uses negative velocity phonons bringing information from the slab on the right.

The discretized PBE, Eq.(19) can be solved in discrete reciprocal space, giving

$$\Phi_Q(q) = -\frac{v_{Qx}\tau_Q(\partial n_Q/\partial T)\nabla_x T(q)}{S(q) + 2i\sin(qd/2)v_{Qx}\tau_Q/d} \quad (20)$$

where $S(q)$ is $\exp(iqd/2)$ if v_{Qx} is positive and $\exp(-iqd/2)$ if v_{Qx} is negative. This gives the answer for the discrete slab gas theory thermal conductivity,

$$\begin{aligned}\kappa(q) &= \frac{1}{\Omega}\sum_Q \hbar\omega_Q\frac{\partial n_Q}{\partial T}v_{Qx}^2\tau_Q\cos(qd/2) \\ &\times\left[\frac{1}{S(q)+2i\sin(qd/2)v_{Qx}\tau_Q/d}\right]\end{aligned} \quad (21)$$

This agrees with the continuum formula Eq.(13) if the small q limit is taken, $\exp(iqd/2)\approx 1\approx\cos(qd/2)$ and $2\sin(qd/2)\approx qd$. Since v_{Qx} changes sign and $S(q)$ becomes $S(q)^*$ when $\vec{Q}$ goes to $-\vec{Q}$, the sum in Eq.(21) is real. Taking the real part of the factor in brackets, Eq.(21) becomes

$$\kappa(q) = \frac{1}{\Omega}\sum_Q \hbar\omega_Q\frac{\partial n_Q}{\partial T}v_{Qx}^2\tau_Q\cos^2(qd/2)F(q,\Lambda_{Qx}) \quad (22)$$

$$F(q,\Lambda) = \left[1 + 4\sin^2(qd/2)\left\{\left(\frac{\Lambda}{d}\right) + \left(\frac{\Lambda}{d}\right)^2\right\}\right]^{-1} \quad (23)$$

where $\Lambda_{Qx} = v_{Qx}\tau_Q$. Now consider what happens at the smallest q, namely $q_{\min} = 2\pi/L$. The factor $\cos^2(q_{\min}d/2) = \cos^2(\pi/N)$ can be set to 1 and $\sin^2(q_{\min}d/2)$ can be set to $(q_{\min}d/2)^2$ when the number N of slabs is large. The correction factor in Eq.(23) becomes, in the large N case,

$$F(q_{\min},\Lambda_{Qx}) \approx \left[1 + \left(\frac{2\pi\Lambda_{Qx}}{L}\right)^2\right]^{-1} \quad (24)$$

The part of Eq.(23) linear in Λ/d is neglected compared to the quadratic part since the correction is only important when $\Lambda/d \gg 1$. Equations 22 and 24 show that when a mean free path $|\Lambda_{Qx}|$ becomes comparable to $L/2\pi$, the contribution of that phonon to $\kappa(q_{\min})$ starts to be suppressed, the suppression becoming complete for phonons Q with $2\pi\Lambda_{Qx} \gg L$. The reason is, if a phonon's mean free path is as large as the period (slab ring circumference), that phonon is now carrying heat from hotter regions to random regions (after cycling around the ring multiple times.) This is a different version of a well-known phenomenon in mesoscale heat transport, where κ in a sample of size L is diminished because long wavelength phonons travel ballistically a shorter distance L, rather than diffusing the longer distance Λ that they would exhibit in bulk[18,19]. Computed behavior based on Eqs. 22 and 23 will be shown in the next section, using a Debye model.

The results developed above enable predictions of $\nabla_x T(\ell+\frac{1}{2})$ and $T(\ell)$ for any given input $\dot{e}(\ell)$. The idea is to use Eqs.(6, 8) to give

$$\begin{aligned}\nabla_x T(\ell+\frac{1}{2}) &= -\sum_{q\neq 0} e^{iqd(\ell+\frac{1}{2})}J_x(q)/\kappa(q) \\ &= -\sum_{q\neq 0} e^{iqd\ell}\frac{\dot{e}(q)d}{(1-e^{-iqd})\kappa(q)},\end{aligned} \quad (25)$$

where the second line follows from the first by using Eq.(18). This can be evaluated using Eq.(21) for $\kappa(q)$. Using Eq.(17), the temperature $T(\ell)$ can also be evaluated, from

$$T(\ell) = T_0 + \sum_{q\neq 0} e^{iqd\ell}\frac{\dot{e}(q)d^2}{4\sin^2(qd/2)\kappa(q)}, \quad (26)$$

where T_0 is the average temperature. The $q=0$ term of these sums is omitted because Eqs.(3,4) make it clear

that $\nabla_x T(q=0) = \sum_\ell \nabla_x T(\ell) = 0$, and similarly for $\dot{e}(q=0)$.

Two approximations have been made. One is the RTA. The other is discretization error. Temperature is a statistical variable, not definable except by averaging over a finite volume. Therefore, discretization over a small width d should not cause noticeable error. However, a problem arises because gas theory has been forced to conform to the slab/junction dichotomy of the discrete picture. This causes the current in the $\ell+\frac{1}{2}$ junction to be tied to the temperature both of the two slabs $\ell+1$ and $\ell+2$ to the right, minus the temperature of both of the two slabs ℓ and $\ell-1$ to the left. This should not be a problem for gas theory, since the theory requires mean free paths longer than the small atomic dimensions used for slab widths. Only if mean free paths are shorter than interatomic spacings (that is, a liquid rather than gas limit) is the current unaware of the temperature beyond the two slabs adjacent to the junction. Nevertheless, a problem arises when the heat input $\dot{e}(\ell)$ is confined to a single site ($\ell = 0$ for example.) Then discretization introduces singular responses in the form of absurd oscillations in the (unphysical) limit of very short mean free path. This problem can be cured by distributing the heat input over three slabs. Specifically, the cure is to use $\dot{e}(\ell) = \dot{e}/2$ when $\ell = 0$, and $\dot{e}/4$ when $\ell = \pm 1$. This modification has more "realism" than a single-site input. Still, it is surprising that it is required in order for gas theory to work smoothly in a slab model. Within the homogeneous slab model, the discrete non-local conductivity (Eq. 5) is an exactly defined concept, as is its Fourier representation $\kappa(q)$. Equations (25,26) are exact connections within linear response, while Eq. 21 uses the PBE, plus a further (and not essential) simplification, the RTA.

V. DEBYE MODEL

Full solution of the PBE, using accurate phonon properties from density functional theory (DFT), is now widely available[20]. Nevertheless, it is useful to have a simplified model as a standard to compare real calculations against. The Debye model replaces the Brillouin zone by a sphere of radius $Q_D = (6\pi^2 n)^{1/3}$, where n is the number of atoms per unit volume. There are three branches of phonons, approximated by $\omega_Q = v|\vec{Q}|$ with the velocity v the same for each branch, and three orthogonal directions $\vec{v}_Q$. The maximum frequency phonon ($\omega_{Q,\max} = \omega_D = vQ_D$) occurs at the edge of the Debye sphere where $|\vec{Q}| = Q_D$. To establish a notation, the specific heat can be written as

$$C(T) = C_\infty \int_0^{\omega_D} d\omega c(\omega) \tag{27}$$

where $c(\omega) = \mathcal{D}(\omega)E(\omega)$, and $C_\infty = 3nk_B$ is the high T classical value of $C(T)$. The factor $\mathcal{D}(\omega)$ is the phonon density of states, normalized to 1. In Debye approximation, this is $\mathcal{D}_\mathcal{D}(\omega) = 3\omega^2/\omega_D^3$. The other factor is $E(\omega) = [(\hbar\omega/2k_BT)/\sinh(\hbar\omega/2k_BT)]^2$, the Einstein formula for the specific heat (in units k_B) of one vibrational mode. This is replaced by the classical limit $E = 1$ ($C(T) = C_\infty$) when comparing with classical MD results.

In the spirit of the Debye model, the mean free path $\Lambda_Q = v\tau_Q$ can be modeled as $\Lambda/\Lambda_{\min}(T) = (Q_D/|\vec{Q}|)^p$, or equivalently, $(\omega_D/\omega)^p$. The exponent p depends on details of scattering. For point impurities such as isotopic substitutions, p takes the Rayleigh value $p = 4$. For "Normal" (N, not Umklapp, or U) anharmonic scattering, Herring[21] found $p = 1$ for transverse and $p = 2$ for longitudinal acoustic modes at low ω. For anharmonic U scattering, which is more relevant here, it is usually argued that $p = 2$, but both $p = 3$ and $p = 4$ have some support from numerical calculations[22,23]. The minimum mean free path, $\Lambda_{\min}$ is found at $|\vec{Q}| = Q_D$. It has a temperature-dependent value, scaling as $1/T$ from anharmonic scattering in the classical high T limit.

First consider the continuum theory. The Debye version has a simple answer in the unphysical case of $p = 0$, where all phonons have the same mean free path, $\Lambda_{\min}$. From Eq.(13), the answer is

$$\kappa_{D,p=0}(k) = \kappa_0(T) g(k\Lambda_{\min}), \tag{28}$$

$$\kappa_{D,p=0}(k \to 0) \equiv \kappa_0(T) = \frac{1}{3} C(T) v \Lambda_{\min}(T). \tag{29}$$

The function $g(k\Lambda_{\min}) = g(u)$ is defined as

$$g(u) = \frac{3}{2}\int_{-1}^{1} d\cos\theta \frac{\cos^2\theta}{1+iu\cos\theta} = \frac{3(u - \tan^{-1} u)}{u^3}. \tag{30}$$

The variable of integration, $\cos\theta$, is the cosine of the angle between the (3d) phonon wavevector $\vec{Q}$ and the direction $\hat{x}$ of the applied temperature gradient. The function $g(u) = \kappa_{D,p=0}(k)/\kappa_0(T)$ is plotted in Fig. 2 for the case where $\Lambda_{\min} = 10d$. In the small k limit, the value is $g \approx 1 - 3u^2/5$.

Eq.(28) for the more physical case of $p > 0$ becomes

$$\frac{\kappa_{D,p}(k)}{\kappa_\infty} = \int_0^{\omega_D} d\omega c(\omega) \left(\frac{\omega_D}{\omega}\right)^p g\left(k\Lambda_{\min}\left(\frac{\omega_D}{\omega}\right)^p\right), \tag{31}$$

where $\kappa_\infty = C_\infty v \Lambda_{\min}(T)/3$ is a convenient scale factor.

For exponent $p \geq 3$, Eq.(31) diverges in the $k \to 0$ limit. The low-ω limit diverges logarithmically at $p = 3$, and more severely at higher p. In theory, the divergence is cut off by finite sample size. This is rarely seen experimentally, since $p = 2$ "N scattering," and Akhieser damping[24,25] provide alternatives. Finite sample size introduces a complication. The boundaries destroy the homogeneity of the theory. Even phonons with k significantly larger than $k_{\min}$ have $\Lambda > L$, and carry heat ballistically, unaware of the spatial variation of sample temperature $T(x)$. To first approximation, this gives a lower limit ($\omega(\Lambda = L)$) below which the integral Eq.(31)

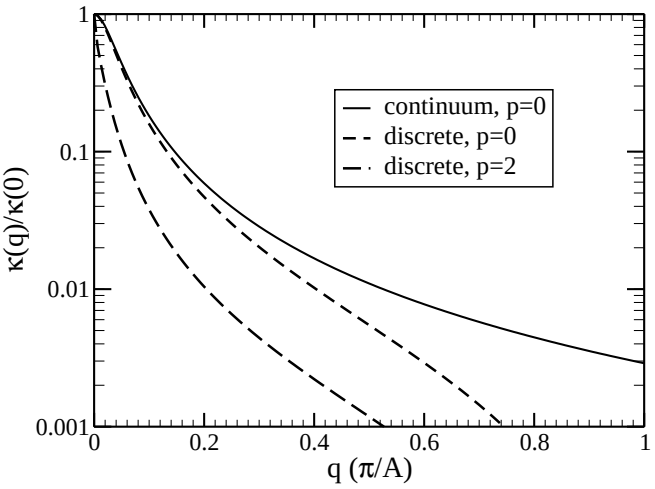

FIG. 2. Thermal conductivity *versus* wavevector, computed in Debye approximation for $\Lambda_{\rm min} = 10d$, and plotted versus wavevector $0 \le q \le \pi/d$. The top curve is the continuum model, Eqs.(28,30) with constant mean free path $\Lambda = \Lambda_{\rm min}$. The middle curve is for the discrete model, Eq.(32) with constant mean free path $p = 0$. The bottom curve, from Eq.(35), uses a more realistic frequency-dependent mean free path, with $p = 2$.

is cut off. Phonons with $\omega_{\rm min} < \omega < \omega(\Lambda = L)$ give ballistic currents, less than their bulk diffusive contribution, and outside the usual local version of the Fourier law. In bulk crystals, this contribution can be important at low T, but not at higher T where such phonons are a very small minority and the ballistic component is negligible.

The Debye model can also be used to find expressions for the non-local conductivity $\kappa(q)$ of the periodic slab model, analogous to $\kappa(k)$ of the continuum model. Note that q and k (discrete and continuous wavevector) are the notational clue indicating the model being solved. First take the unphysical model with constant mean free path ($p = 0$). Using Eq.(21), the analog of Eq.(28) is

$$\kappa_{D,p=0}(q) = \kappa_0(T) h'(q, \Lambda_{\rm min}) = \kappa_0(T) h(w) \qquad (32)$$

where $h'(q, \Lambda_{\rm min}) = h(w)$ is

$$h(w) = \frac{3\cos(qd/2)}{2} \left[\int_0^1 d\cos\theta \frac{\cos^2\theta}{e^{iqd/2} + iw\cos\theta} + \int_{-1}^0 d\cos\theta \frac{\cos^2\theta}{e^{-iqd/2} + iw\cos\theta} \right]. \qquad (33)$$

Here $w = 2\sin(qd/2)\Lambda_{\rm min}/d$ is the discretized version of $u = k\Lambda_{\rm min}$ that appears in Eq.(30). Note that, although h depends separately on q and on $\Lambda_{\rm min}$, the additional q-dependence beyond that contained in w plays only the role of a fixed parameter, while the w dependence acquires additional importance when the mean-free path Λ_Q acquires ω_Q-dependence.

Performing the $d\cos\theta$ integral gives

$$h(w) = \frac{3\cos(qd/2)}{w^3} {\rm Re}\left\{ we^{iqd/2} + ie^{iqd} \ln\left[1 + iwe^{-iq/d2}\right] \right\}. \qquad (34)$$

This reduces to Eq.(30) in the small q limit, under the replacements $q \to k$ and $w \to u$. The function $h = \kappa_{D,p=0}(q)/\kappa_0(T)$ is also shown in Fig. 2. Up until $q \approx 0.2\pi/d$ ($q \approx 2\pi/\Lambda_{\rm min}$) the discrete and continuum versions fall almost equally rapidly with q to < 0.1. Beyond, the discrete case falls increasingly rapidly, going to 0 at the zone boundary, $q = \pm\pi/d$. This means, for example, that there is no response to input heating $\dot{e}(\ell) = \dot{e}\exp(\pm i\pi\ell) = (-1)^\ell \dot{e}$. The reason is that adjacent junctions have currents $J(\ell + \frac{1}{2}) = \pm\dot{e}/2$. Therefore, the slab current (the average of the two adjacent junction currents) is zero.

For the more physical case of $p > 0$, the answer is

$$\frac{\kappa_{D,p}(q)}{\kappa_\infty} = \int_0^{\omega_D} d\omega c(\omega) \left(\frac{\omega_D}{\omega}\right)^p h\left(q\Lambda_{\rm min}\left(\frac{\omega_D}{\omega}\right)^p\right) \qquad (35)$$

The function $\kappa_{D,p=2}(q)/\kappa_\infty$ is shown in the classical limit ($c(\omega) = \mathcal{D}(\omega)$) in Fig. 2 as the bottom curve. The conductivity falls more much rapidly with q, which means increased non-locality. This is not surprising. Spatial memory extends much farther because of the longer mean free paths. These results are translated back to coordinate space in Fig. 3. The $p = 0$ (constant Λ) results fall exponentially (as $\exp(-md/\Lambda)$) if the supercell size Nd exceeds Λ sufficiently. The $p = 2$ case behaves differently. At a distance $md = 8\Lambda_{\rm min} = 80d$, the value of $\kappa(m)$ is $\approx \kappa(0)/8.4$, falling much more slowly than an exponential.

VI. NUMERICAL RESULTS

Fig. 4 illustrates the computed spatial temperature variation for the discrete slab model. The behavior closely resembles that found by Zhou *et al.*[13] in their classical MD simulation of GaN. Therefore, I believe that the PBE, as extended here to discrete slabs, and modeled in RTA and in the Debye approximation, correctly captures the physics. The calculations of Fig. 4 use the classical limit $C(T) = C_\infty$, with mean free path $\Lambda = \Lambda_{\rm min}(\omega_D/\omega)^2$, $\Lambda_{\rm min} = 20d$, and various total cell lengths L ranging from $40d$ to $2560d$. Symmetry requires $T(N/4 + m) = -T(N/4 - m)$, and an inflection point in $T(\ell)$ at $\ell = N/4$. At the largest N shown, the distance $N/4$ between heat input and sink is $32\Lambda_{\rm min}$, and the answer for $\kappa_{\rm eff}(N)$ is still 10% lower than the macroscopic ($N \to \infty$) limit. The temperature profile is accurately linear, over the 60 slabs shown, for the three largest lengths L, but the slopes are 10 to 30% higher than the macroscopic limit.

Zhou *et al.*[13] invoke a Mattheissen's rule justification for extrapolation to $L \to \infty$, namely the idea that "boundary scattering" causes $1/\kappa$ to behave like

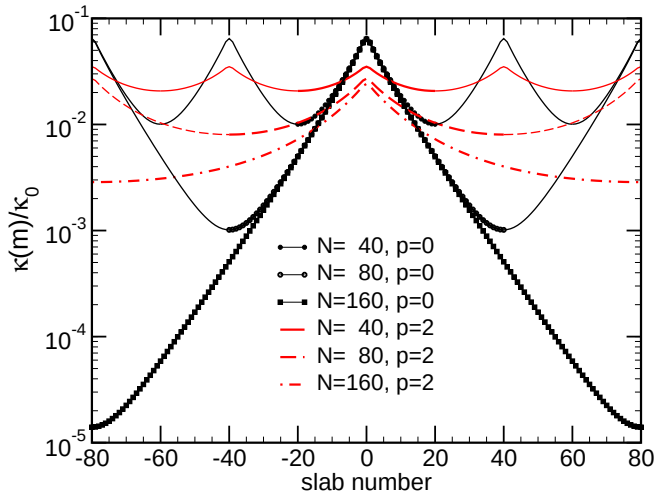

FIG. 3. The non-local thermal conductivity, $\kappa(m)$ defined in Eq.(5), and computed using Eq.(35) for the slab model, Fourier transformed back to coordinate space. The minimum mean free path $\Lambda_{\min}$ is $10d$; the supercell has N slabs of width d, where N is shown in the figure legend. The period N repetitions are shown. Black and red curves use the power law $p = 0, 2$ respectively of $\Lambda_Q = \Lambda_{\min}(\omega_D/\omega_Q)^p$.

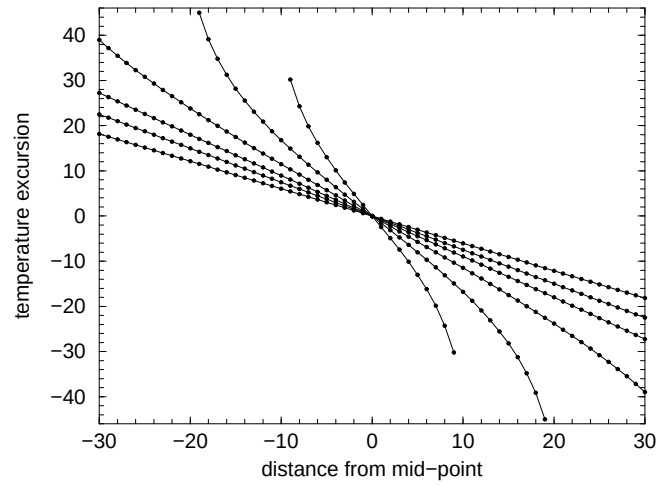

FIG. 4. Temperature *versus* distance from the midpoint $\ell = N/4$ between hot ($\ell = 0$) and cold ($\ell = N/2$) points. All computations used the discrete slab formula (Eq.(35)) and $\Lambda_{\min} = 20d$. The power law $1/\tau_Q$ is ω_Q^2. The cell size N was 40 for the steepest curve, then 80, 160, 320, 640, and 2560.

$1/\Lambda + 1/L$. However, their cell has periodic boundary conditions and therefore no actual boundary. The discrete version of the PBE presented here uses correct statistical theory and incorporates the ring geometry by design. Therefore, it should correctly describe the rate at which $\kappa_{\text{eff}}(L)$ converges to the $L \to \infty$ limit, and provide guidance for extrapolation. Fig. 5 shows how $\kappa_{\text{eff}}(L)$ converges as L increases. Models with constant mean

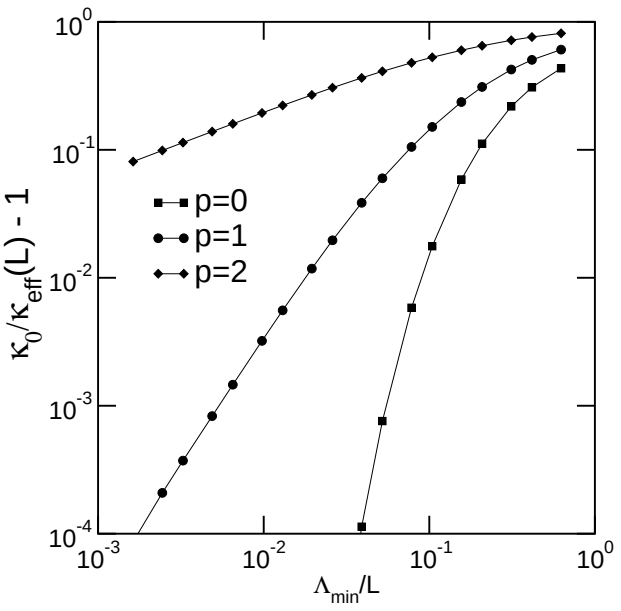

FIG. 5. Rate of convergence of $1/\kappa_{\text{eff}}(L)$ to its $L \to \infty$ limit, by a logarithmic plot as a function of Λ_{min}/L. All computations used the discrete slab formula (Eq.(35)) and $\Lambda_{\min} = 10$. From bottom to top, the power law p of $1/\tau_Q \propto \omega_Q^p$ is $p = 0$, 1, and 2. The numerical power law of $\kappa_0/\kappa - 1 \propto (1/L)^s$ is $s \approx \infty$, 2, and 1/2.

free path converge exponentially, as $\exp(-4\Lambda/L)$. This is true both for continuum and discrete cases. This is not surprising, but I have not yet found a simple proof. The factor of 4 just relates to the fact that only 1/4 of the ring ($\Delta m = N/4$) is available for decay. Discrete models with mean free paths diverging as $1/\omega$ ($p = 1$) and $1/\omega^2$ ($p = 2$) are also shown in Fig. 5. They apparently converge algebraically, as $1/L^2$ for $p = 1$ and $1/\sqrt{L}$ for $p = 2$. These powers were found numerically from the slope of the log-log graphs. I conjecture that the behavior is $\kappa_{\text{bulk}} - \kappa_{\text{eff}}(L) \propto (1/L)^{(3-p)/p}$. This scaling for $p = 2$ is in rough accord with the highest temperature simulation by Zhou *et al.*[13], where convergence was nonlinear in $1/L$. A plot of their numerical results *versus* $1/\sqrt{L}$ instead of $1/L$ gives a significantly better straight line. Unfortunately, the extrapolated value then falls below $1/\kappa = 0$, indicating that even larger simulation cells are needed before extrapolation can be relied on. Results for GaN by Lindsay *et al.*[26], using DFT and PBE, agree well with experiment. They also show that isotopically pure GaN will have $\kappa(300K) \approx 400$W/mK. This indeed makes $1/\kappa$ closer to 0 than to the extrapolated values of Zhou *et al.*.

VII. DISCUSSION

Non-local heat transport is seldom explicitly[1] discussed. The non-locality is hidden if the temperature

gradient is uniform. Then the form of the non-locality (contained in $\kappa(k)$ for a homogeneous system) is irrelevant, since only the $k \to 0$ limit is seen. The PBE contains a valid description of non-local response, provided the carrier mean free path is sufficiently long that a quasiparticle gas description is valid. The work described in this paper uses phonon gas theory, as contained in the PBE, to describe the non-locality. The PBE is reformulated for finite size systems with periodic boundary conditions. Discretization into parallel slabs is natural for one-dimensional transport. The resulting $\kappa(q)$ (Eq.(35)) has, I believe, negligible discretization error, and correctly includes the nanoscale corrections that enter when mean free paths are comparable to the simulation cell length L in an MD simulation. This situation is hard to avoid for materials with good crystalline order and weak anharmonicity, such as the GaN simulation of ref. 13.

Picturing heat transport as explicitly non-local may have benefits. For example, in MD simulations of κ by the "direct method," it would be sensible to impose heat in a periodic fashion, $\dot{e}(\ell) = \cos(2\pi\ell/N)$, or $\dot{e}(q)$ containing only the smallest non-zero $q = 2\pi/Nd$ allowed. This simplifies Eqs.(25,26). More important, it should enable extrapolation to the $q \to 0$ limit more smoothly. Equally important, it should help reduce the noise level of MD simulations, because the "measured" $T(\ell)$ would be used at all ℓ to extract $T(q)$, rather than using only a few points of $T(\ell)$ to extract a gradient at the midpoint. A future paper on this topic is planned.

A number of recent papers formulate theories of heat conductivity in nanoscale systems[27–30]. Microscopic theory is needed, not just to supplement simulation, but more importantly, to aid experiment in interpreting nanoscale effects. Non-local effects are evident in heat transport by nanoscale samples of good conductors like graphene. Landauer methods[31–33] are often preferred, but have limitations when inelastic scattering is present. Meir-Wingreen-type[34] approaches often used to supplement Landauer methods in electron transport, and can be generalized to heat transport[28]. The PBE, which is evidently useful to model non-locality, and includes inelasticity, can perhaps be exploited in new ways to simplify and unify some of these problems.

VIII. ACKNOWLEDGEMENTS

This work was suggested by discussions with M.-V. Fernandez-Serra and J. Siebert, whose stimulation is gratefully acknowledged. I also thank D. Broido, G. Chan, Y. Li, K. K. Likharev, J. Liu, A. J. H. McGaughey, S. Ocko, T. Sun, R. M. Wentzcovitch, and an anonymous referee for helpful input. This work was supported in part by DOE grant No. DE-FG02-08ER46550.

* philip.allen@stonybrook.edu

[1] G. D. Mahan and F. Claro, Phys. Rev. B **38**, 1963 (1988).
[2] C. Dames and G. Chen, Thermal Conductivity of Nanostructured Thermoelectric Materials, CRC Handbook, edited by M. Rowe (Taylor and Francis, Boca Raton, FL, 2006), Ch. 42.
[3] G. Chen, *Nanoscale energy Transport and Conversion* (Oxford University Press, Oxford, 2005), Ch. 7.
[4] Z. M. Zhang, *Nano/Microscale Heat Transfer* (McGraw-Hill, New York, 2007), Ch. 5.
[5] D. G. Cahill, W. K. Ford, K. E. Goodson, G. D. Mahan, A. Majumdar, H. J. Maris, R. Merlin, and S. R. Phillpot, J. Appl. Phys. **93**, 793 (2003).
[6] A. Majumdar, J. Heat Transfer **115**, 7 (1993).
[7] J. A. Johnson, A. A. Maznev, J. Cuffe, J. K. Eliason, A. J. Minnich, T. Kehoe, C. M. Sotomayor Torres, G. Chen, and K. A. Nelson, Phys. Rev. Lett. **110**, 025901 (2013).
[8] A. A. Maznev, J. A. Johnson, and K. A. Nelson, Phys. Rev. B **84**, 195206 (2011).
[9] K. C. Collins, A. A. Maznev, Z. Tian, K. Esfarjani, K. A. Nelson, and G. Chen, J. Appl. Phys. **114**, 104302 (2013).
[10] D. N. Payton, M. Rich, and W. M. Visscher, Phys. Rev. **160**, 706 (1967).
[11] F. Müller-Plathe, J. Chem. Phys. **106**, 6082 (1997).
[12] A. Maiti, G. D. Mahan, and S. T. Pantelides, Solid State Commun. **102**, 517 (1997).
[13] X. W. Zhou, S. Aubry, R. E. Jones, A. Greenstein, and P. K. Schelling, Phys. Rev. B **79**, 115201 (2009).
[14] B.-Y. Cao and Y.-W. Li, J. Chem. Phys. **133**, 024106 (2010).
[15] D. P. Sellan, E. S. Landry, J. E. Turney, A. J. H. McGaughey, and C. H. Amon, Phys. Rev. B **81**, 214305 (2010).
[16] R. Peierls, Ann. Phys. **3**, 1055 (1929).
[17] J. M. Ziman, *Electrons and Phonons* (Oxford University Press, London, 1960).
[18] A. J. Minnich, Phys. Rev. Lett. **109**, 205901 (2012).
[19] C. Hua and A. J. Minnich, Phys. Rev. B **89**, 094302 (2014).
[20] W. Li, J. Carrete, N. A. Katcho, and N. Mingo, Computer Phys. Commun. **185**, 1747 (2014).
[21] C. Herring, Phys. Rev. **95**, 954 (1954).
[22] A. Ward and D. A. Broido, Phys. Rev. B **81**, 085205 (2010).
[23] K. Esfarjani, G. Chen, and H. T. Stokes, Phys. Rev. B **84**, 085204 (2011).
[24] A. Akhieser, J. Phys. (USSR) **1**, 277 (1939).
[25] H. J. Maris, in *Physical Acoustics*, edited by W. P. Mason and R. N. Thurston (Academic, New York, 1971), Vol. 8, p. 279.
[26] L. Lindsay, D. A. Broido, and T. L. Reinecke, Phys. Rev. Lett. 109, 095901, (2012)
[27] G. Lebon, H. Machrafi, M. Grmela, and Ch. Dubois, Proc. R. Soc A **467**, 3241 (2011).
[28] S. G. Das and A. Dhar, Eur. Phys. J. B **85**, 372 (2012).
[29] K. Sääskilahti, J. Oksanen, and J. Tulkki, Phys. Rev. E **88**, 012128 (2013).
[30] F. Yang and C. Dames, Phys. Rev. b **87**, 035437 (2013).

[31] R. Landauer, Z. Phys. B - Condensed Matter **68**, 217 (1987).
[32] D. E. Angelescu, M. C. Cross, and M. L. Roukes, Superlattices Microstruct. **23**, 673 (1998).
[33] N. Mingo, Phys. Rev. B **68**, 113308 (2003).
[34] Y. Meir and N. S. Wingreen, Phys. Rev. Lett. **68**, 2512 (1992).